

S.M. CRISTESCU^{1,✉}
S.T. PERSIJN^{1,*}
S. TE LINTEL HEKKERT²
F.J.M. HARREN¹

Laser-based systems for trace gas detection in life sciences

¹ Life Science Trace Gas Facility, Molecular and Laser Physics, Institute for Molecules and Materials, Radboud University, P.O. Box 9010, 6500 GL Nijmegen, The Netherlands
² Sensor Sense BV, P.O. Box 9010, 6500 GL Nijmegen, The Netherlands

Received: 21 January 2008/Revised version: 30 June 2008
Published online: 1 August 2008 • © The Author(s) 2008

ABSTRACT Infrared gas phase spectroscopy is becoming very common in many life science applications. Here we present three types of trace gas detection systems based on CO₂ laser and continuous wave (cw) optical parametric oscillator (OPO) in combination with photoacoustic spectroscopy and cw quantum cascade laser (QCL) in combination with wavelength modulation spectroscopy. Examples are included to illustrate the suitability of CO₂ laser system to monitor in real time ethylene emission from various dynamic processes in plants and microorganisms as well as from car exhausts. The versatility of an OPO-based detector is demonstrated by simultaneous detection of ¹³C-methane and ¹²C-methane (at 3240 nm) at similar detection limits of 0.1 parts per billion by volume. Recent progress on a QCL-based spectrometer using a continuous wave QCL (output power 25 mW, tuning range of 1891–1908 cm⁻¹) is presented and a comparison is made to a standard chemiluminescence instrument for analysis of NO in exhaled breath.

PACS 42.62 Be; 42.62 Fi

1 Introduction

Infrared gas phase spectroscopy is nowadays very common in a wide variety of real life applications. For monitoring industrial processes, air pollution, global warming, security in public places or biological processes in living organisms (including the human body) laser-based spectroscopic gas sensors have demonstrated to be indispensable tools [1–4]. They operate in the infrared wavelength region between 2.5 and 20 μm, where many of the molecules of interest have their fundamental rovibrational transitions. Laser-based sensors combine a high detection sensitivity (at the pptv level, parts per trillion by volume; 1 : 10¹²) with selectivity, large dynamic range and multicomponent analysis.

However, an important limiting element in those sensors is the laser source itself; there is a limited availability of wavelength, low power, restricted tunability, large linewidth, etc. In the mid-infrared, available laser sources include line-tunable CO and CO₂ lasers, lead-salt diode lasers, tunable solid-state

lasers, quantum and interband cascade lasers, and coherent sources such as optical parameter oscillators (OPO) and difference frequency generation (DFG) systems. Any breakthrough for laser-based gas sensors will largely depend on the access to proper laser sources at low cost, besides compactness, reliability and the ability to operate under various atmospheric conditions.

Lasers such as the CO laser and the lead-salt laser are difficult to incorporate into a commercial device because of their need for cryogenic cooling. Non-linear generation of infrared light via DFG or OPO (based on periodically poled lithium-niobate (PPLN) crystals) provide a broad continuous tuning range (hundreds of wavenumbers) [5–8]. However, DFG is inherently restricted to low powers (up to few mW) [3, 9–11], to reach the ppbv level of sensitivity with such low powers, advanced detection schemes are needed. OPOs have relatively high power levels (1 W cw) and narrow linewidth (typically a few MHz over 1 s) and, therefore, represent an excellent source for sensitive spectroscopic gas analysis. In combination with fiber pump laser technology the OPO-based sources offer the attractive advantage of a rather compact set-up. However, up to now OPOs are less suitable for field applications as the cavity needs occasional tweaking.

Until a few years ago, direct generation of tunable mid-infrared radiation using solid-state lasers suffered especially from limited output power, low temperature operation and limited tuning properties. However, there have been major recent advances to the development of high power solid state quantum cascade lasers (QCL) operating at room temperature. Therefore, these lasers are very interesting in terms of system integration [12].

To unravel highly dynamic processes in life sciences there is an increasing demand for real time measurements of trace gases emissions, molecule specificity and no need for sample preparation. Capturing all details of emission patterns requires instruments which combine a high sensitivity at mostly pptv levels at a seconds' time scale resolution. Such a goal can be achieved in two ways: (1) By using high power lasers in combination with simple, robust, and easy to maintain detection schemes. One example of such an instrument is the CO₂ laser-based photoacoustic detector for monitoring ethylene (C₂H₄) emission [13]; the CO₂ laser lines shows a strong overlap with the Q-branch of the ν₇-band of ethylene [14]. This CO₂ laser-based ethylene detector, today commercially

✉ Fax: +31 (0)24 365 33 11, E-mail: simona@science.ru.nl

*Present address: NMI Van Swinden Laboratorium B.V., Delft, The Netherlands

available as a compact 19-inch rack design [15], performs as the world's best instrument for sensitive and fast detection of the plant hormone ethylene. (2) When high power sources are not available, other spectroscopic techniques are used to achieve high performances in terms of sensitivity and time response such as cavity ring down spectroscopy (CRDS), cavity enhanced absorption spectroscopy (CEAS), integrated cavity output spectroscopy (ICOS), and multi-pass absorption spectroscopy (in combination with wavelength modulation schemes). We have explored various detection methods in combination with different laser sources for trace gas detection: photoacoustic spectroscopy (PAS) in combination with CO lasers [16], CO₂ lasers [17] and OPO [18], cavity enhanced absorption spectroscopy with CO₂ laser [19], quartz enhanced photoacoustic spectroscopy (QEPAS) with OPO [20], CRDS using OPO [21, 22] and wavelength modulation spectroscopy (WMS) with OPO [23] and QCL [24].

In our laboratory we have developed a long-standing tradition of cooperation with life science research groups via European Union visiting programs [25]. From these cooperations it is demonstrated that laser-based systems are indispensable for trace gas detection in many life science fields including plant physiology, post harvest research, soil science, environment, microbiology, entomology, ecology, molecular biology, medicine, and human health. Here, we illustrate the performance of several trace gas detection systems based on CO₂ laser, OPO and QCL, respectively with examples of application in various life science areas.

2 Ethylene monitoring with a CO₂ laser-based photoacoustic detector

There are numerous reports on the capability of CO₂ laser-based photoacoustic systems in detecting gaseous molecules (SF₆, NH₃, ozone, etc.) [2]. In particular for the plant hormone ethylene, the use of such a detector in combination with a flow-through system was proven to be unbeatable in sensitivity and time response in comparison to the traditional methods (such as gas chromatography which is currently the standard technique most widely used). A detailed description of the system is given elsewhere [2, 13, 26]. Briefly, the laser-based ethylene detector consists of a CO₂ laser and a photoacoustic cell, in which the gas is detected. Traces of ethylene released by various (biological) samples can absorb the laser radiation inside the photoacoustic cell; the absorbed energy is released as heat, which will create a pressure increase inside a closed volume. By modulating the laser at an acoustic frequency, a periodic pressure wave is generated that can be detected with a sensitive miniature microphone. The ethylene concentration is calculated from comparison of the photoacoustic signals on various laser lines (at which ethylene has different absorption strengths). The laser-based instrument allows detection of ethylene emission in a continuous flow system down to 10 pptv over 90 s [26]. In photoacoustic spectroscopy (PAS), use of a high power (preferably a watt level) coherent light source (such as the CO₂ laser) is necessary in order to reach sub-ppbv detection levels. The combination of PAS and the CO₂ laser has resulted in simple, robust and easy to maintain designs which are giving PAS a competitive advantage over other sensitive techniques (e.g.

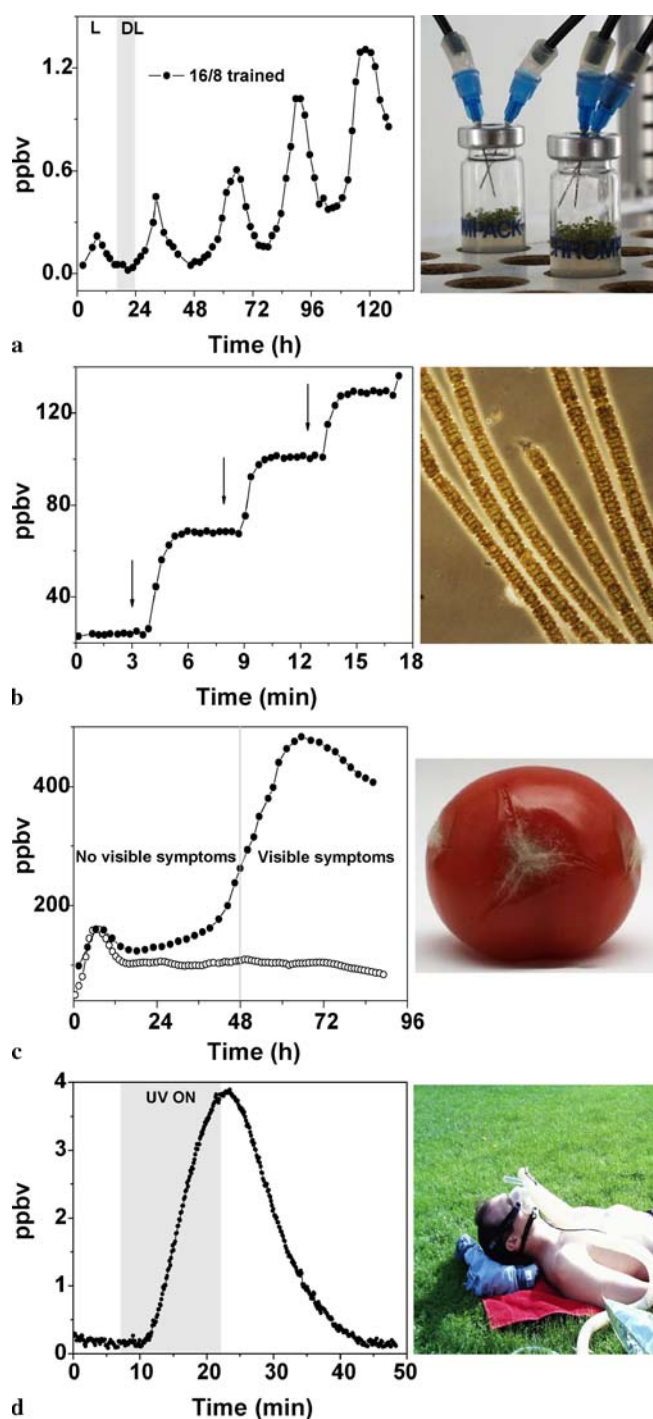


FIGURE 1 Ethylene production from various biological samples. (a) Plant physiology: circadian clock in *Arabidopsis thaliana* with a peak in the mid-subjective day; (b) Microbiology: response of cyanobacteria *N. spumigena* to changing the light intensities (indicated by arrows) from dark to 5, 10 and 25 $\mu\text{mol m}^{-2} \text{s}^{-1}$, respectively; (c) Post harvest technology: early detection of *B. cinerea* (grey mold) infection in tomato fruits. Real time production by artificially inoculated tomato fruits (at $t = 0$ h) with *B. cinerea* (●) starts rising one day before visible infection as compared to uninfected fruit injected with water (○); (d) Medicine: on line emission from human breath induced by UV radiation

cavity ring-down spectroscopy, cavity enhanced absorption spectroscopy, etc.).

Over the last few years, we have used the laser-based ethylene systems within the life science trace gas facility for on-

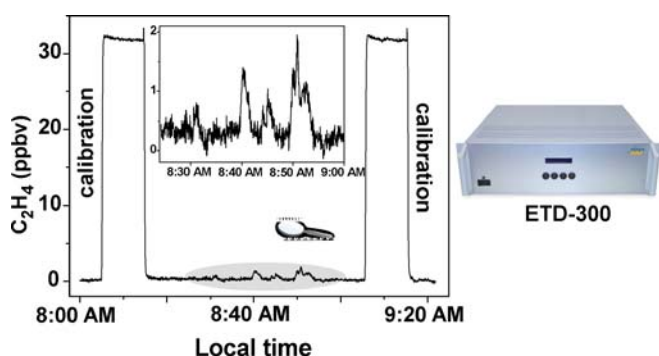


FIGURE 2 Real time monitoring of ethylene concentration in a parking place at the NOAA facility in Boulder, Colorado (*left panel*). Outside air was pumped into the laboratory through 3/8 inch PFA tubing and analyzed with the laser-based commercial ethylene detector ETD-300, Sensor Sense (*right panel*). The peaks in the inset are attributed to vehicles in the immediate vicinity of the sampling inlet around morning on a working day

line measurement of ethylene in various dynamic processes in plants and microorganisms, such as seed germination [27], flower senescence [28], fruit ripening [29], circadian rhythm in plants (Fig. 1a) [30], nitrogen fixation (Fig. 1b) [31, 32], plant–pathogen interaction (Fig. 1c) [33, 34], plant response to insect egg deposition [35], interaction with other plant hormones, i.e. auxin [36], dehydration and drought [37, 38], programmed cell death [39], hypertensive disorders of pregnancy [40], and UV-induced damage to skin (Fig. 1d) [41, 42].

More applications appear at the horizon once the development of these detectors move on from the laboratory systems to the field instruments. A very recent project focused on the detection of ethylene emission from car exhaust (Fig. 2) at ground level following the same sampling procedure as described in [43]. Another study revealed and quantified ethylene fluxes from petrochemical zones around Houston, TX (USA) during flight campaigns using CO₂ laser based ethylene detector (Sensor Sense) that achieves a noise equivalent minimum detection limit of 70 pptv within a 5 s observation time [44].

3 Detection of ¹³CH₄ using OPO-based system

Recently, cw OPOs were developed to a level that they combine high power (> 1 W) with a broad tuning range (2.75–3.83 μm) and narrow line width (4.5 MHz over 1 s) [18, 21]. For trace gas detection purposes they are combined with photoacoustic spectroscopy. An excellent detection limit of 0.01 ppbv for ethane at 2996.9 cm⁻¹ was obtained by scanning over the absorption peak in 40 s [45]. The extension of the OPO wavelength to 4.2 μm brought a strong CO₂ absorption in range, offering a sensitivity of 7 ppbv (0.3 s RC-time, measured at the top of the peak) which made it possible to monitor the breath of a small ant [46].

A recent application of the OPO system included monitoring of ¹²CH₄ and ¹³CH₄ emissions by plants. The study was provoked by an earlier study published in Nature [47] containing a sparking finding that terrestrial plants can produce a large amount of methane in aerobic conditions. In collaboration with other research groups we have re-examined this finding using an independent test [48]. For this study we used ¹³C labeled plants grown in controlled conditions in an experi-

mental soil plant atmosphere system (ESPAS) facility [49]. The ESPAS is a unique hermetically sealed plant growth chamber (3.5 m³), specifically designed for atmospheric isotope labeling. Four plants species (basil, wheat, maize and sage) were labeled (IsoLife BV, Wageningen, The Netherlands) from seeds on hydroponics for a period of nine weeks in ¹³C-CO₂ (99% ¹³C, 1% ¹²C) instead of the natural atmospheric ¹²C-CO₂ concentration (1.1% ¹³C, 98.9% ¹²C). Since about 99% of the carbon found in these plants was in the form of ¹³C (data not shown) we can expect that nearly 99% of the methane emitted by these plants is in the form of ¹³C-methane. When investigating possible methane emission, it is preferable to use these ¹³C labeled plants since the natural background concentration of ¹³C-methane is 20 ppbv compared to 1.7 ppmv of ¹²C-methane.

After 7–8 weeks of growth in the ESPAS growth chamber, the plants were transferred to continuous-flow gas exchange cuvettes and on-line analyzed for ¹³C-methane emission. Additionally, gas samples from the ESPAS facility were collected in Tedlar and aluminum-coated Teflon bags and sent to the laboratory for methane measurements.

The experimental set-up is shown in Fig. 3. The singly-resonant OPO is pumped by a 1064 nm MOPA system (Lightwave M6000) that can generate as much as 11 W of output power. The pump laser can be continuously tuned over 48 GHz by means of a piezo. The OPO cavity consists of a bowtie ring design using a 50 mm MgO-doped PPLN crystal (HC Photonics) and can generate as much as 2.8 W of idler power [45]. The idler wavelength is measured by a wavelength meter (model 621, Bristol Instruments). The idler beam is amplitude modulated by a chopper at 560 Hz and directed to the photoacoustic cell (length resonator of 300 mm, diameter of 6 mm) which is equipped with three electret microphones.

Methane shows a very pronounced absorption spectrum around 3000 cm⁻¹ which is dominated by the strong ν₃ band [50, 51]. Since both ¹³CH₄ and ¹²CH₄ molecules are spherical rotors, their spectra are similar but shifted by about 10 cm⁻¹ due to the difference in the carbon mass [52]. For the detection of ¹³CH₄ the lines around 3240 nm were se-

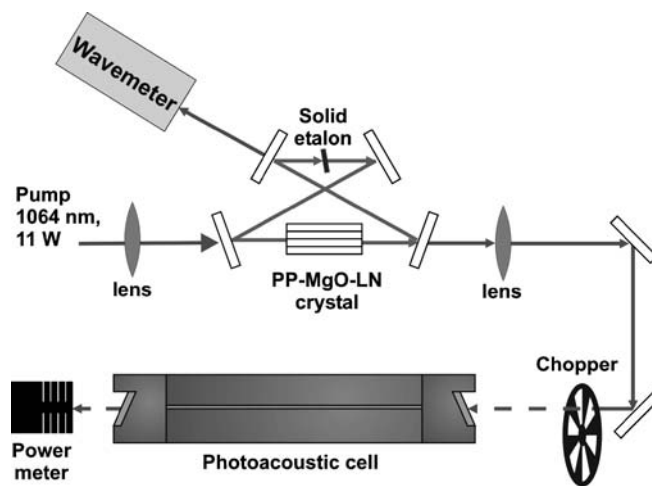


FIGURE 3 Experimental set-up of the cw singly resonant OPO-based PAS system. The OPO cavity consists of four mirrors in a bowtie ring design, using a 50 mm MgO-doped PPLN crystal. The idler beam is amplitude modulated by a chopper at 560 Hz and directed to the photoacoustic cell

lected based on several criteria. The water vapor absorption strength at this wavelength is a factor $\sim 10^6$ weaker than methane. Furthermore, the absorption features of $^{13}\text{CH}_4$ and $^{12}\text{CH}_4$ are sufficiently separated from each other at a photoacoustic cell pressure of 250 mbar and the $^{13}\text{CH}_4$ absorption is relatively strong. To subtract interferences from $^{12}\text{CH}_4$, the OPO was scanned over a wider wavelength range of 0.5 nm. A noise-equivalent detection limit of 0.1 ppbv for $^{12}\text{CH}_4$ was found. The absorption strength of $^{13}\text{CH}_4$ is about the same order of magnitude as for $^{12}\text{CH}_4$, thus enriched mixtures of $^{13}\text{CH}_4$ were detected with the same sensitivity. However, at the natural background concentration (20 ppbv $^{13}\text{CH}_4$), an accuracy of 3 ppbv for $^{13}\text{CH}_4$ is obtained (within 1 min response time) [21, 45].

We measured on-line an overall average concentration of $21 \text{ ng g}^{-1} \text{ h}^{-1}$ ^{13}C -methane which is 6–18 times lower than the average methane emission rates given in [47] for the same plant species under “sunlight” and “no sun” conditions, respectively. Furthermore, within a six day period, the total plant biomass in the ESPAS growth chamber increased from 289 to 374 g DW. Based on the measured average methane emission of $21 \text{ ng g}^{-1} \text{ h}^{-1}$ in our on-line experiment and the plant biomass in the growth chamber, we expected to measure 495 ppbv ^{13}C -methane in the gas samples collected in bags from ESPAS at the end of this period, a value well above our detection limit.

In reality, we found an increase over time of less than 1 ppbv ^{13}C -methane (Fig. 4), which is only 0.1 and 0.3% respectively of the emissions that would have been expected on the basis of the rates under ‘sunlight’ and ‘no sun’ conditions reported in [47].

Additional tests were performed to eliminate the possibility of eventual $^{13}\text{CH}_4$ loss because of leakage or oxidation. For this purpose a known amount of $^{13}\text{CH}_4$ (40 ppb, 1.5 ppm, 100 ppm) was injected in the ESPAS chamber and gas samples were analyzed (Fig. 4). Furthermore, 400 ppbv of $^{13}\text{CH}_4$ was injected into the growth chamber and air samples were taken over a period of six days from the ESPAS (Fig. 5). All these samples were then measured and showed a non-significant concentration decrease of 0.3%.

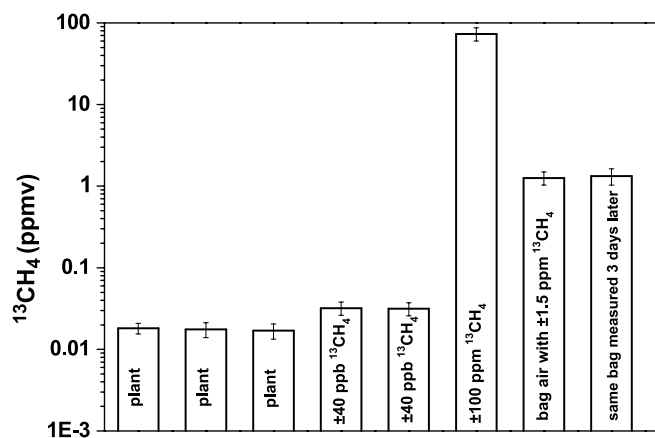


FIGURE 4 Measurements of $^{13}\text{CH}_4$ concentration in the samples collected from the ESPAS chamber containing the plants. Additional amount of $^{13}\text{CH}_4$ (40 ppb, 1.5 and 100 ppm) was injected in the ESPAS chamber to check for eventual $^{13}\text{CH}_4$ losses

The results from these tests indicate the same conclusion that plants produce an insignificant methane amount in aerobic conditions [48]. We have also performed on-line measurements of $^{12}\text{CH}_4$ from “normal” plants (not ^{13}C labeled) placed into closed cuvettes and flushed with methane-free air before starting the experiment as well as during it. The only methane recorded (Fig. 6) was due to the flushing out of the atmospheric methane trapped in the plant cells for several hours. This could explain, in part, the overestimated methane reported in [47] as production instead of atmospheric methane diffusion from plant tissue.

4 Nitric oxide detection with a QCL-based spectrometer

Detection of nitric oxide (NO) at trace levels is of major importance for medical, biological and environmental applications. In plants NO is a key signaling molecule which acts against oxidative stress and in addition plays a role in plant pathogen interactions [53, 54]. For humans, the presence

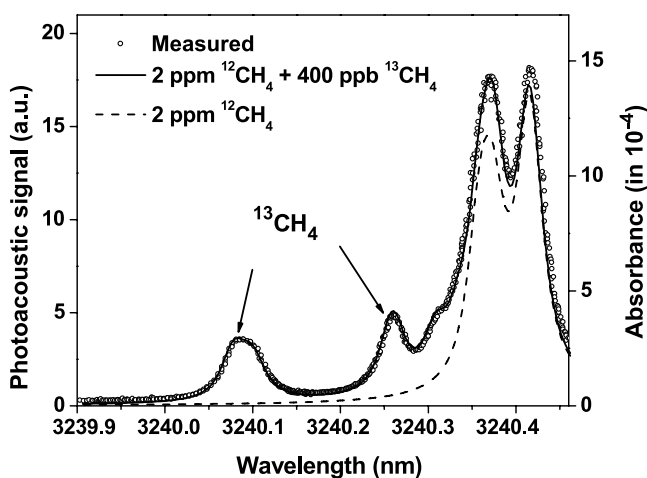


FIGURE 5 Methane spectra. Calculated spectra from the Hitran database (<http://cfa-www.harvard.edu/Hitran>) for 2 ppm $^{12}\text{CH}_4$ (dashed line) and 2 ppm $^{12}\text{CH}_4$ enriched with 400 ppm $^{13}\text{CH}_4$ (solid line). Measured spectrum of 2 ppm $^{12}\text{CH}_4$ enriched with 400 ppm $^{13}\text{CH}_4$ (\circ) injected in the ESPAS facility for testing possible loss of $^{13}\text{CH}_4$

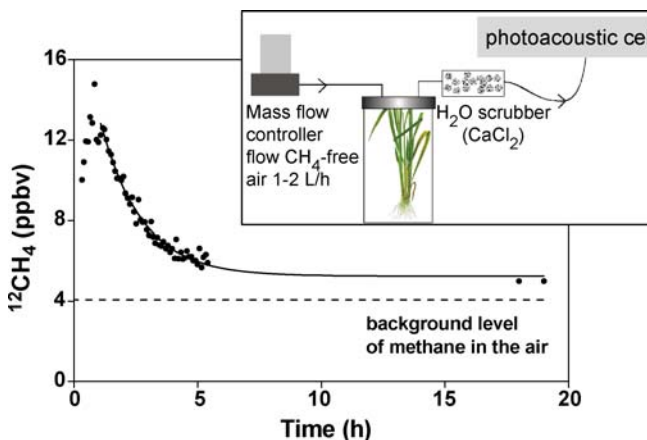


FIGURE 6 Diffusion of atmospheric methane trapped in the plant cells. *Upper panel:* on line photoacoustic monitoring of $^{12}\text{CH}_4$ from plants flushed with methane free air at high flow (1 l/min) for 1 h before the start ($t = 0$ h) and at 1–2 l/h during the experiment; water is reduced by inserting a CaCl_2 scrubber

of endogenous NO in the exhaled air was observed for the first time in 1991 [55] and since then exhaled NO was found to be a sensitive marker for (asthmatic) airway inflammation [56].

The standard technique to measure NO in the gas phase is by chemiluminescence which features a high sensitivity at the sub-ppbv level in combination with a time response of less than one second [57]. A drawback of this technique is the use of chemical scrubbers which need to be replaced on a regular basis. In addition, most systems are designed for rather high flow rates of typically a few hundred milliliters per minute, which renders them suitable for breath measurements but less suitable for certain biological applications where relatively small flow rates are needed [54].

An alternative way to measure NO is via infrared absorption-based detection techniques that use the fundamental absorption band of NO centered at $5.3 \mu\text{m}$ (1876 cm^{-1}) [58]. This method was used more than 35 years ago by Kreuzer and Patel, who were able to detect concentrations of 0.01 ppm NO using CO laser-based photoacoustics [59]. The recent advances of thermo-electrically cooled QCLs operating in the NO fundamental absorption band gave a strong impulse to the development of QCL-based NO detectors [24, 60, 61]. Here we present recent progress on a QCL-based spectrometer and its application to human breath analysis.

The QCL-based spectrometer is equipped with an astigmatic multi-pass absorption cell (Fig. 7) for wavelength modulation spectroscopy on NO. The set-up underwent several modifications compared to our previous design [24]. Firstly, a new cw DFB QCL (Alpes Lasers) with a higher output power (25 mW) and tuning range of $1891\text{--}1908 \text{ cm}^{-1}$ as compared to 5 mW and $1847\text{--}1854 \text{ cm}^{-1}$ of the old laser, was used. CO_2 absorption is markedly stronger in the $1891\text{--}1908 \text{ cm}^{-1}$ wavelength region [58] and CO_2 levels as found in breath can be measured simultaneously with NO using only current scanning. The QCL is cooled with a Peltier element to a temperature of -30°C . Unfortunately, the output beam quality of the QCL is rather poor showing several diffraction rings. Various mirrors and lenses are used to direct the output beam to a 76-m astigmatic multi-pass absorption cell (Aerodyne, AMAC-76). To facilitate long-term unattended operation the liquid nitrogen cooled HgCdTe

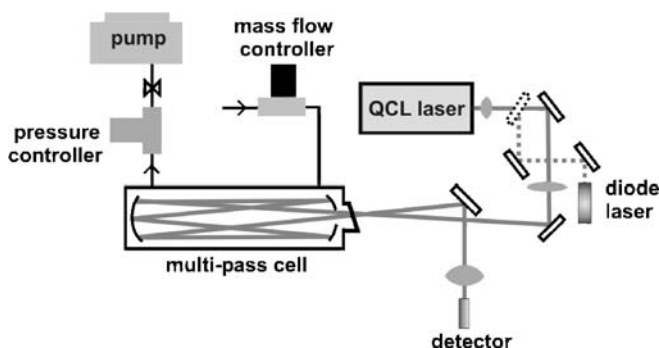


FIGURE 7 Schematic set-up of the cw QCL-based detector. The output beam of the QCL is collimated using a ZnSe lens (0.5 inch focal length) and focused by a second ZnSe lens ($f = 45 \text{ cm}$) in the astigmatic multiple-pass absorption cell. A diode laser is used as a tracer beam by inserting a mirror on a flip mount. After leaving the absorption cell, the light is focused by a CaF_2 lens ($f = 15 \text{ cm}$) onto the detector. The detector signal is fed into a lock-in amplifier and the $2f$ signal is sent to a computer via a fast digitizer for data acquisition

photodiode detector has been replaced by a photovoltaic detector operating at room temperature (PV-6, Vigo System, $D \geq 4 \times 10^8 \text{ cm Hz}^{1/2}/\text{W}$). Detector noise was not limiting in our system as a comparable sensitivity was obtained for both detectors although the sensitivity of the new detector is two orders of magnitude smaller. The whole system is enclosed in a box flushed with dry nitrogen to prevent condensation of water vapor from the surrounding air on the QCL.

The laser current is swept at a frequency of 200 Hz on top of which a 125 kHz modulation is superimposed. The detector signal is pre-amplified and sampled at twice the modulation frequency by a lock-in amplifier (model SR844, Stanford Research Systems) using a time constant of $100 \mu\text{s}$ and filter roll-off of 24 dB/oct.

The wavelength scans were stored using a fast 14-bit data acquisition card (Gage Compuscope 14200). The width of the scan is typically 0.25 cm^{-1} . A narrower range ($\sim 0.06 \text{ cm}^{-1}$) could be used if only the NO peak would be measured. The pressure in the multi-pass cell is maintained at 100 mbar using a combination of pressure controller and pump. At lower pressures the system becomes more sensitive to temperature drifts while at higher pressures spectral interference by a neighboring CO_2 absorption line comes into play.

For the data analysis a LabVIEW program has been developed which allows on-line concentration measurements. To start with, the signals are recorded from the background and a calibration mixture with known concentration of 100 ppbv NO (NMI, the Netherlands). The NO concentration in a sample is determined by correlating (an average of) scans of the sample with the scan of the known concentration in which both scans are corrected for the background. The slope of a linear fit yields the concentration relative to the known concentration. A similar procedure can be done for CO_2 . This approach yields several advantages as compared to the previously used fitting method based on the second derivative of a pseudo-Voigt. The new fitting procedure is much more rapid. In addition, the second derivative fit is not optimal as the $2f$ signal is not symmetric. The new fitting procedure is suitable to fit any line shape, symmetric or not.

Wavelength fluctuations in the order of a few thousands of a wavenumber occur due to temperature instabilities. As

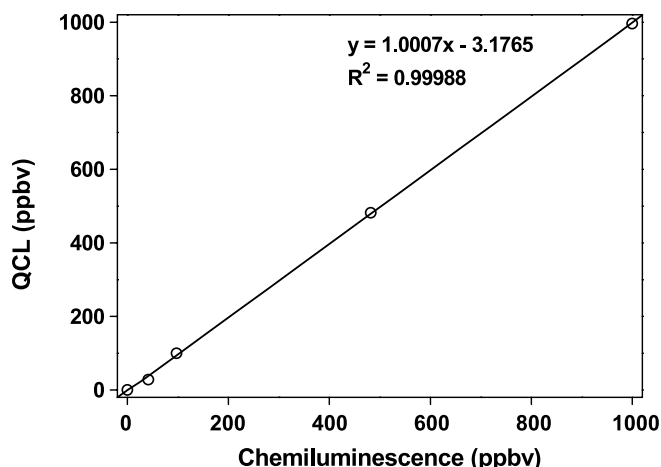


FIGURE 8 Comparison between NO concentrations measured by the QCL-based NO detector and the NO chemiluminescence detector

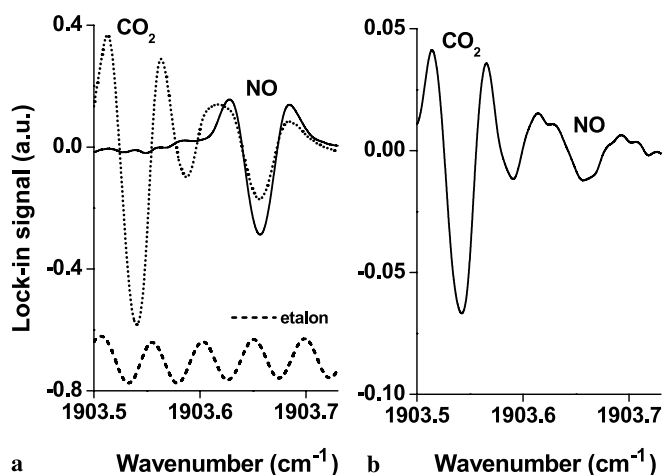


FIGURE 9 Scan over NO and CO₂ absorption lines around 1903 cm⁻¹. (a) Measurement of a mixture of 50% CO₂ and 500 ppbv NO (solid line) and 1 ppmv NO (dotted line). At the bottom an etalon trace is shown (free spectral range 0.049 cm⁻¹). (b) Breath measurement revealing a CO₂ concentration of 5.8% and NO concentration of 34 ppbv (chemiluminescence 30 ppbv)

a result the absorption peaks are shifted as compared to the trigger signal. However the distance between the peak of NO and the (much higher) CO₂ peak is almost constant. By using this CO₂ peak as a reference the system becomes much less sensitive to temperature fluctuations. The system was operated by averaging 400 scans (~ 3 s) giving a sensitivity of the system of 1 ppbv. The system response was compared to a commercial NO analyzer based on chemiluminescence (Sievers 280). The response of both detectors (Fig. 8) is nearly identical. The instrument was applied to the detection of NO and CO₂ in human breath. Breath samples were taken off-line by blowing against a restriction and collecting the sample in balloons [62]. Samples were directly afterwards measured by chemiluminescence and the QCL-based spectrometer. Figure 9a shows measurements of a mixture of CO₂ and NO diluted in nitrogen and of only NO diluted in nitrogen. Frequency markers are provided by the etalon trace. In Fig. 9b a breath sample is displayed. A CO₂ concentration of 5.8% is found which is typical for human breath. The NO concentration of 34 ppb corresponds well with the value found by chemiluminescence of 30 ppbv.

At the moment, optical fringing limits the system sensitivity to 1 ppbv. We plan to improve the system's performance by using a set of lenses internal in the QCL housing to improve the beam quality and so reduce fringing. A clear advantage of this NO detection system is that no liquid nitrogen cooling is required, neither for the laser source nor the detector, making long-term experiments feasible as needed e.g. in plant biology [54].

5 Conclusions and future outlook

Three different cw light sources have been presented here i.e. CO₂ laser, OPO, and QCL in combination with two detection techniques namely photoacoustic spectroscopy and wavelength modulation spectroscopy. Applications from different fields of life science demonstrate their potential for laboratory and field experiments, respectively. For detecting a single species, the CO₂ laser remains a powerful

source especially in combination with PAS. The QCLs seem very promising because of their wavelength tailorability over a wide spectral range in the mid-infrared (to far-infrared), increasing output powers (already exceeding 100 mW at certain wavelengths), operation at room temperature and great potential for compact design. With further increases in QCL output powers, photoacoustic spectroscopy can be a cheaper, more robust and simpler alternative compared to multi-pass absorption cells or cavity ring down related schemes. The current cw OPO systems available in our lab are suitable to detect only a few species simultaneously due to the 'limited' pump scanning range of 48 and 150 GHz [20, 21], respectively. Wider scans are in principle possible by changing the crystal temperature or by gradually changing poling period using a fan out grating. However, this approach is not suitable for long-term stand-alone operation as occasional realignment is necessary due to thermal effects. Widely tunable OPOs have been demonstrated [63, 64] although in general with relatively large line widths. If wide tunability and frequency agility can be combined with a narrow line width, OPO-based instruments may once replace currently operated analytical instruments like FTIRs or gas chromatographs.

ACKNOWLEDGEMENTS The authors would like to thank to Danny Ramsamoedj (RUN, Nijmegen) for developing the software for data-acquisition and analysis, Peter Steenberg and Jan van Amsterdam (RIVM, Amsterdam) for lending us the chemiluminescence NO analyzer. NMI (Delft) for providing us with the NO calibration mixture. Joost de Gouw and Carsten Warneke (NOAA, Bolder) for monitoring ethylene emission from cars. Financial support from the Dutch Technologiëstichting STW and the European Commission (FAIR grant CT98-4211, "Fruta Fresca"; FP6-NESTA-0025042, "The Optical Nose"; EU-FP6-Infrastructures-5, FP6-026183 'Life Science Trace Gas Facility').

OPEN ACCESS This article is distributed under the terms of the Creative Commons Attribution Noncommercial License which permits any noncommercial use, distribution, and reproduction in any medium, provided the original author(s) and source are credited.

REFERENCES

- 1 M.W. Sigrüst, *Rev. Sci. Instrum.* **74**, 486 (2003)
- 2 F.J.M. Harren, G. Cotti, J. Oomens, S. te Lintel Hekkert, In: *Encyclopedia of Analytical Chemistry*, ed. by R.A. Meyers (Wiley, New York, 2000)
- 3 F.K. Tittel, D. Richter, A. Fried, In: *Solid-state Mid-infrared Laser Sources*, ed. by I.T. Sorokina, K.L. Vodopyanov (Springer, Berlin, 2003)
- 4 M. Mürtz, D. Halmer, M. Horstjann, S. Thelen, P. Hering, *Spectrochim. Acta A* **63**, 963 (2006)
- 5 M.M.J.W. van Herpen, S.E. Bisson, A.K.Y. Ngai, F.J.M. Harren, *Appl. Phys. B* **78**, 281 (2004)
- 6 S.E. Bisson, K.M. Armstrong, T.J. Kulp, M. Hartings, *Appl. Opt.* **40**, 6049 (2001)
- 7 F. Müller, A. Popp, F. Kühnemann, S. Schiller, *Opt. Express* **11**, 2820 (2003)
- 8 M.E. Klein, C.K. Laue, D.H. Lee, K.J. Boller, R. Wallenstein, *Opt. Lett.* **25**, 490 (2000)
- 9 S.E. Bisson, T.J. Kulp, O. Levi, J.S. Harris, M.M. Fejer, *Appl. Phys. B* **85**, 199 (2006)
- 10 W.D. Chen, E. Pouillet, J. Burie, D. Boucher, M.W. Sigrüst, J.J. Zondy, L. Isaenko, A. Yelissev, S. Lobanov, *Appl. Opt.* **44**, 4123 (2005)
- 11 D. Richter, P. Weibring, *Appl. Phys. B* **82**, 479 (2006)
- 12 F.K. Tittel, Y. Bakhirkin, A.A. Kosterev, G. Wysocki, *Rev. Laser. Eng.* **34**, 275 (2006)
- 13 F.J.M. Harren, J. Reuss, In: *Encyclopedia of Applied Physics*, ed. by G.L. Trigg (VCH, Weinheim, 1997), Vol. 19
- 14 R.J. Brewer, C.W. Bruce, J.L. Mater, *Appl. Opt.* **21**, 4092 (1982)

- 15 <http://www.sensor-sense.nl>
- 16 F.G.C. Bijnen, H. Zuckermann, F.J.M. Harren, J. Reuss, *Appl. Opt.* **37**, 3345 (1998)
- 17 F.J.M. Harren, L.J.J. Laarhoven, In: *Optics Encyclopedia*, ed. by T.G. Brown, K. Creath, H. Kogelnik, M.A. Kriss, J. Schmit, M.J. Weber (Wiley-VCH, Weinheim, 2004)
- 18 A.K.Y. Ngai, S.T. Persijn, M.M.J.W. van Herpen, S.M. Cristescu, F.J.M. Harren, In: *Mid-infrared Coherent Sources and Applications*, ed. by M. Ebrahim-Zadeh, I.T. Sorokina (Springer, Dordrecht, 2007)
- 19 R. Peeters, G. Berden, A. Olafsson, L.J.J. Laarhoven, G. Meijer, *Chem. Phys. Lett.* **337**, 231 (2001)
- 20 A.K.Y. Ngai, S.T. Persijn, I.D. Lindsay, A.A. Kosterev, P. Gross, C.J. Lee, S.M. Cristescu, F.K. Tittel, K.J. Boller, F.J.M. Harren, *Appl. Phys. B* **89**, 123 (2007)
- 21 A.K.Y. Ngai, S.T. Persijn, G. von Basum, F.J.M. Harren, *Appl. Phys. B* **85**, 173 (2006)
- 22 A.K.Y. Ngai, H. Verbraak, S.T. Persijn, H. Linnartz, F.J.M. Harren, *Appl. Phys. Lett.* **90**, 081 109 (2007)
- 23 S.T. Persijn, A.K.Y. Ngai, F.J.M. Harren, I.D. Lindsay, P. Gross, B. Adhimoollam, K.J. Boller, In: *Proc. of CLEO Europe, München, 17–22 June 2007*, paper CD3-6-MON
- 24 B.W.M. Moeskops, S.M. Cristescu, F.J.M. Harren, *Opt. Lett.* **31**, 823 (2006)
- 25 <http://cordis.europa.eu/infrastructures/>
- 26 F.G.C. Bijnen, J. Reuss, F.J.M. Harren, *Rev. Sci. Instrum.* **67**, 2914 (1996)
- 27 A. Gianinetti, L.J.J. Laarhoven, S.T. Persijn F.J.M. Harren, L. Petruzzelli, *Ann. Bot.* **99**, 735 (2007)
- 28 C. Wagstaff, U. Chanasut, F.J.M. Harren, L.J. Laarhoven, B. Thomas, H.J. Rogers, A.D. Stead, *J. Exp. Bot.* **56**, 1007 (2005)
- 29 P.M.M. Iannetta, L.J. Laarhoven, N. Medina-Escobar, E.K. James, M.T. McManus, H.V. Davies, F.J.M. Harren, *Physiol. Plant.* **127**, 247 (2006)
- 30 S.C. Thain, F. Vandenbussche, L.J.J. Laarhoven, M.J. Dowson-Day, Z.Y. Wang, E.M. Tobin, F.J.M. Harren, A.J. Millar, D. van der Straeten, A.J. Millar, *Plant Physiol.* **136**, 3751 (2004)
- 31 M. Staal, S. te Lintel Hekkert, F. Harren, L.J. Stal, *Environ. Microbiol.* **3**, 343 (2001)
- 32 M. Staal, S. te Lintel Hekkert, G.J. Brummer, M. Veldhuis, C. Sikkens, S. Persijn, L.J. Stal, *Limnol. Oceanogr.* **52**, 1305 (2007)
- 33 S.M. Cristescu, E.J. Woltering, F.J.M. Harren, In: *Food Mycology, a Multifaceted Approach to Fungi and Food*, ed. by J. Dijksterhuis, R.A. Samson (CRC Press, New York, 2007)
- 34 C. Montero, J.B. Jiménez, J.M. Orea, A. González Urea, S.M. Cristescu, S. te Lintel Hekkert, F.J.M. Harren, *Plant Physiol.* **131**, 129 (2003)
- 35 R. Schröder, S. Cristescu, F. Harren, M. Hilker, *J. Exp. Bot.* **58**, 1835 (2007)
- 36 F. van den Bussche, J. Smalle, J. Le, N.J. Madeira Saibo, A. de Paepe, L. Chaerle, O. Tietz, R. Smets, L.J.J. Laarhoven, F.J.M. Harren, H. van Onckelen, K. Palme, J.-P. Verbelen, D. van der Straeten, *Plant Physiol.* **131**, 1228 (2003)
- 37 O. Leprince, F.J.M. Harren, J. Buitink, M. Alberda, F.A. Hoekstra, *Plant Physiol.* **122**, 597 (2000)
- 38 M. Balota, S. Cristescu, W.A. Payne, S. te Lintel Hekkert, L.J.J. Laarhoven, F.J.M. Harren, *Crop Sci.* **44**, 812 (2004)
- 39 E.T. Yakimova, V.M. Kapchina-Toteva, L.J. Laarhoven, F.M. Harren, E.J. Woltering, *Plant Physiol. Biochem.* **44**, 581 (2006)
- 40 P.L.M. Zusterzeel, R.P.M. Steegers-Theunissen, F.J.M. Harren, E. Stekinger, H. Kateman, B.H. Timmerman, R. Berkelmans, A. Nieuwenhuizen, W.H.M. Peters, M.T.M. Raijmakers, E.A.P. Steegers, *Hypertens. Pregnancy* **21**, 39 (2002)
- 41 F.J.M. Harren, R. Berkelmans, K. Kuiper, S. te Lintel Hekkert, P. Scheepers, P. Hollander, R. Dekhuijzen, D.H. Parker, *Appl. Phys. Lett.* **74**, 1761 (1999)
- 42 B.W.M. Moeskops, M.M.L. Steeghs, K. van Swam, S.M. Cristescu, P.T.J. Scheepers, F.J.M. Harren, *Physiol. Meas.* **27**, 1187 (2006)
- 43 W.C. Kuster, F.J.M. Harren, J. de Gouw, *Environ. Sci. Technol.* **39**, 1157 (2005)
- 44 J.A. de Gouw, C. Warneke, S. te Lintel Hekkert, J.S. Holloway, D.D. Parrish, J. Peischl, T.B. Ryerson, J. Mellqvist, E.A. Atlas, A. Fried, In: *Proc. of 2007 Fall Meeting of the American Geophysical Union, 10–14 December, 2007*, paper A131-06
- 45 M.M.J.W. van Herpen, S. Li, S.E. Bisson, F.J.M. Harren, *Appl. Phys. Lett.* **81**, 1157 (2002)
- 46 M.M.J.W. van Herpen, A.K.Y. Ngai, S.E. Bisson, J.H.P. Hackstein, A.J. Woltering, F.J.M. Harren, *Appl. Phys. B* **82**, 665 (2006)
- 47 F. Keppler, J.T.G. Hamilton, M. Brass, T. Rockmann, *Nature* **439**, 187 (2006)
- 48 T. Dueck, R. de Visser, H. Poorter, S. Persijn, A. Gorissen, W. de Visser, A. Schapendonk, J. Verhagen, J. Snel, F.J.M. Harren, A.K.Y. Ngai, F. Verstappen, H. Bouwmeester, L.A.C.J. Voeseek, A. van der Werf, *New Phytol.* **175**, 29 (2007)
- 49 A. Gorissen, P.J. Kuikman, J.H. Van Ginkel, H. Van de Beek, A.G. Jansen, *Plant Soil* **179**, 81 (1996)
- 50 R.A. Toth, L.R. Brown, R.H. Hunt, L.S. Rothman, *Appl. Opt.* **20**, 932 (1981)
- 51 L. Fejard, J.P. Champion, J.M. Jouvard, L.R. Brown, A.S. Pine, *J. Mol. Spectrosc.* **201**, 83 (2000)
- 52 C.R. Webster, *Appl. Opt.* **44**, 1226 (2005)
- 53 M.V. Beligni, L. Lamattina, *Plant Cell Environ.* **24**, 267 (2001)
- 54 L.A.J. Mur, I.E. Santosa, L.J.J. Laarhoven, N.J. Holton, F.J.M. Harren, A.R. Smith, *Plant Physiol.* **138**, 1247 (2005)
- 55 L.E. Gustafsson, A.M. Leone, M.G. Persson, N.P. Wikuld, S. Moncada, *Biochem. Biophys. Res. Commun.* **181**, 852 (1991)
- 56 M.J. Lanz, D.Y.M. Leung, D.R. McCormick, R. Harbeck, S.J. Szeffler, C.W. White, *Pediatr. Pulmonol.* **24**, 305 (1997)
- 57 D. Yao, A.G. Vlessidis, N.P. Evmiridis, *Microchim. Acta* **147**, 1 (2004)
- 58 L.S. Rothman, D. Jacquemart, A. Barbe, D.C. Benner, M. Birk, L.R. Brown, M.R. Carleer, C. Chackerian, K. Chance, L.H. Coudert, V. Dana, V.M. Devi, J.M. Flaud, R.R. Gamache, A. Goldman, J.M. Hartmann, K.W. Jucks, A.G. Maki, J.Y. Mandin, S.T. Massie, J. Orphal, A. Perrin, C.P. Rinsland, M.A.H. Smith, J. Tennyson, R.N. Tolchenov, R.A. Toth, J. Vander Auwera, P. Varanasi, G. Wagner, *J. Quant. Spectrosc. Radiat. Transf.* **96**, 139 (2005)
- 59 L.B. Kreuzer, C.K.N. Patel, *Science* **173**, 47 (1971)
- 60 D.D. Nelson, J.H. Shorter, J.B. McManus, M.S. Zahniser, *Appl. Phys. B* **75**, 343 (2002)
- 61 Y.A. Bakhirkin, A.A. Kosterev, R.F. Curl, F.K. Tittel, D.A. Yarekha, L. Hvozdar, M. Giovannini, J. Faist, *Appl. Phys. B* **82**, 149 (2006)
- 62 J.G.C. van Amsterdam, A.P.J. Verlaan, H. van Loveren, S.G. Vos, A. Opperhuizen, P.A. Steerenberg, *Int. Arch. Occup. Environ. Health.* **72**, 404 (1999)
- 63 M.E. Klein, P. Gross, K.J. Boller, M. Auerbach, P. Wessels, C. Fallnich, *Opt. Lett.* **28**, 920 (2003)
- 64 M.M.J.W. van Herpen, S.E. Bisson, A.K.Y. Ngai, F.J.M. Harren, *Appl. Phys. B* **78**, 281 (2004)